

# In Silico Designing, ADMET Screening, MM/GBSA Binding Free Energy of Some Novel 8-Amino Substituted Apigenin Derivatives as DPP-IV Inhibitors Targeting Type-II Diabetes Mellitus

Ritika Sahu<sup>1\*</sup>, Surendra Jain<sup>2</sup>, Deepti Jain<sup>3</sup>

<sup>1\*</sup>,<sup>3</sup>School Of Pharmaceutical Sciences, Rajiv Gandhi Proudyogiki Vishwavidyalaya, Airport Road, Bhopal, MP, 462033

<sup>2</sup>Truba Institute of Pharmacy, Karond-Gandhi Nagar Bypass Road, Bhopal, MP, 462038

\*Corresponding Author: - Ritika Sahu

\*School Of Pharmaceutical Sciences, Rajiv Gandhi Proudyogiki Vishwavidyalaya, Airport Road, Bhopal, MP, 462033

E-Mail:- ritikasahu15@gmail.com

DOI: 10.47750/pnr.2022.13.S05.418

## Abstract

Diabetes has long been a major issue for the world's health. Drugs for hypoglycemia are now administered orally and intravenously, however they have several toxic and adverse consequences. Therefore, there is an increasing demand to find anti-diabetic medications that are more potent and secure. Since it was discovered that apigenin is an edible, plant-derived flavonoid with no toxicity, scientists have been quite concerned. Plants are rich sources of apigenin (API), a well-known insulin-secretagogue and insulin-mimetic substance. Incretin enhancers known as dipeptidyl peptidase-IV (DPP-IV) inhibitors are used to treat diabetes. It is necessary to produce new agents, ideally from natural sources, with less negative consequences due to their unpleasant side effects. The purpose of this in-silico design process was to create new 8-Amino substituted apigenin derivatives (RSMS 1–50) with DPP-IV inhibitory action. Using Schrodinger suit 2020-3, docking studies of molecules RSMS1–50 are carried out against DPP-IV (PDB id–6B1E). The Glide module, the QikProp module, and the Prime-MMGBSA module of the Schrodinger suit are used to execute the molecular docking research for the designed compounds RSMS1–50. Based on the GLIDE score, the binding affinity of the proposed molecules RSMS 1–50 towards DPP-IV was selected. Many substances demonstrated effective hydrogen bonding and hydrophobic communication to obstruct DPP-IV enzyme. Comparing the compounds RSMS1-50 to conventional Vildagliptin (- 5.3) and Sitagliptin (- 5.6), they show significant Glide scores between - 4.32 and - 8.39. The proposed information concerning drug similarity includes the in-silico ADMET characteristics. The most potent inhibitor has positive MM-GBSA binding. The findings demonstrate that 8-Amino substituted apigenin derivatives should be taken into account as possible DPP-IV inhibitors. Further in vitro and in vivo studies may demonstrate the therapeutic potential of the substances, RSMS 10, 15, 35, 26, 30, 45, and 47 with substantial Glide scores.

**Keywords:** MM-GBSA, DPP-IV, In-silico ADMET screening, Docking investigations.

## INTRODUCTION

Type-2 diabetes commonly referred to as adult-onset diabetes or non-insulin-dependent diabetic mellitus (NIDDM), makes up 90–95% of all instances of the disease. Type-2 diabetes often appears in people after the age of 45, and the chance of developing it rises with age. However, type 2 diabetes in youngsters is becoming more and more common. Due to macrovascular disease and microvascular long-term consequences, diabetes is very prevalent and is linked with increased mortality and morbidity [1, 2]. Therefore, effective treatment strategies for glycaemic management are very necessary. The pharmacological family of glucose-lowering drugs known as dipeptidylpeptidase-4 (DPP-4) inhibitors offers new opportunities for the treatment of type 2 diabetes (T2DM). These medications increase the levels of the incretin hormones glucagon-like peptide-1 (GLP-1) and glucose-dependent insulin tropic polypeptide by inhibiting the DPP-4 enzyme, which quickly converts two important gastrointestinal hormones into inactive by products (GIP). DPP-4 inhibitors have a different mechanism of action than any other family of oral glucose-lowering medications in the market [3]. Although DPP-4 inhibitors result in comparable reductions in blood glucose levels and glycated haemoglobin (HbA1c) levels, they have a number of therapeutic benefits [4]. A newer pharmacological family of glucose-lowering drugs known as dipeptidyl peptidase-4 (DPP-4) inhibitors offers new possibilities for the treatment of type 2 diabetes mellitus (T2DM). DPP-4 inhibitors have a different mechanism of action than any other family of oral glucose-lowering medications now on the market [5]. Although DPP-4 inhibitors do not have a greater ability to reduce blood glucose levels or glycated haemoglobin (HbA1c) levels, they do have a number of clinically significant benefits [6–8]. A weight-neutral profile in contrast to the weight increase often seen with SU and thiazolidinedione, and a minimal risk of hypoglycaemia that is far lower than that reported with sulphonyl urea (SU) are two of the most significant advantages (TZD). DPP-4 inhibitors have been tested both alone and in various combinations with other

glucose-lowering medications, and they have been put up against a placebo or a medication from a different pharmacological class as an active comparator [9]. One of the most prevalent non-mutagenic, non-toxic flavonoids (subclass- Flavone) is apigenin (5,7-dihydroxy-2-(4-hydroxyphenyl) chromen-4-one) and is found in plants like *Cynodon dactylon*, chamomile, and others. Numerous studies have noted apigenin's antioxidant qualities, coupled with its anti-hyperglycaemic, anti-inflammatory, and (in myocardial ischemia) anti-apoptotic activities. Flavonoids are generally well recognised for their antioxidant characteristics. [10] In mice injected with A25-3515, apigenin is shown to be neuroprotective, increasing blood-brain barrier integrity, learning, and memory, as well as providing neurovascular protection. Apigenin is a strong antioxidant that may increase insulin production from the pancreas and the transport of glucose in peripheral tissues. It also has the ability to lengthen the half-life of incretin hormones [11–15]. In the present study, we target the DPP-IV enzyme using API as an incretin enhancer and analyse its potential anti-diabetic and DPP-IV inhibitory effects using *in silico* methods. The findings demonstrated that the newly constructed 8-Amino substituted apigenin derivatives displayed significant inhibition of diabetes mellitus with the DPP-4 enzyme.

## MATERIAL AND METHODS

### Molecular docking studies

#### Protein preparation

The DPP-IV enzyme with co-crystallized ligand (PDB ID: 6B1E, 1.77 Å) was recovered from the protein data bank. The protein was built up using the Protein Preparation Wizard module of Schrödinger Suite 2020-3. Using the Schrödinger suite 2020-3 prime module, missing chain atoms are added. The protein heteroatom was given potential ionisation states, and the most steady-state candidate was chosen. In order to reorient side-chain hydroxyl groups and prevent possible steric conflicts, the protein structure energy was finally minimised under controlled conditions [16–21]. Dipeptidyl peptidase-4 (DPP-4), commonly referred to as the T-cell antigen CD26, is a multifunctional protein that serves as a binding protein and ligand for several extracellular compounds in addition to its catalytic activity. It is a crucial membrane protein that is expressed on cells throughout the body, but it is also expelled from the membrane and circulates in the plasma as a soluble protein. DPP-4 has been shown to cleave a vast number of bioactive compounds *in vitro*, although only a small number of them have been shown to have physiological substrates. One of them is the incretin hormone glucagon-like peptide-1 (GLP-1), which has been demonstrated to be the major enzyme controlling its biological activity [22–25]. GLP-1 plays a significant role in maintaining proper glucose homeostasis. The DPP-4 protein has a long intracellular tail at the N-terminus and a large extracellular domain that is fixed in the cell membrane by a flexible region connected to a trans-membrane sequence (Figure 2). The extracellular domain, which circulates in the plasma as "soluble" DPP-4 but is also present in other body fluids including seminal fluid and cerebrospinal fluid, may be cleaved at the stalk however, the extracellular domain of the protein has a cysteine-rich area and a region rich in glycosylation sites in addition to the catalytic site, which is located in the C-terminal portion of the extracellular domain. These regions are thought to play a significant role in the majority of DPP-4 non-enzymatic activities, interacting with proteins like adenosine deaminase, caveolin-1, streptokinase, and plasminogen, as well as with extracellular matrix elements like collagen and fibronectin, and serving as binding sites for molecules like the chemokine CXCR4 receptor, the T-cell differentiation antigen CD45, and the sodium-hydrogen exchanger-3, among others [26-27].

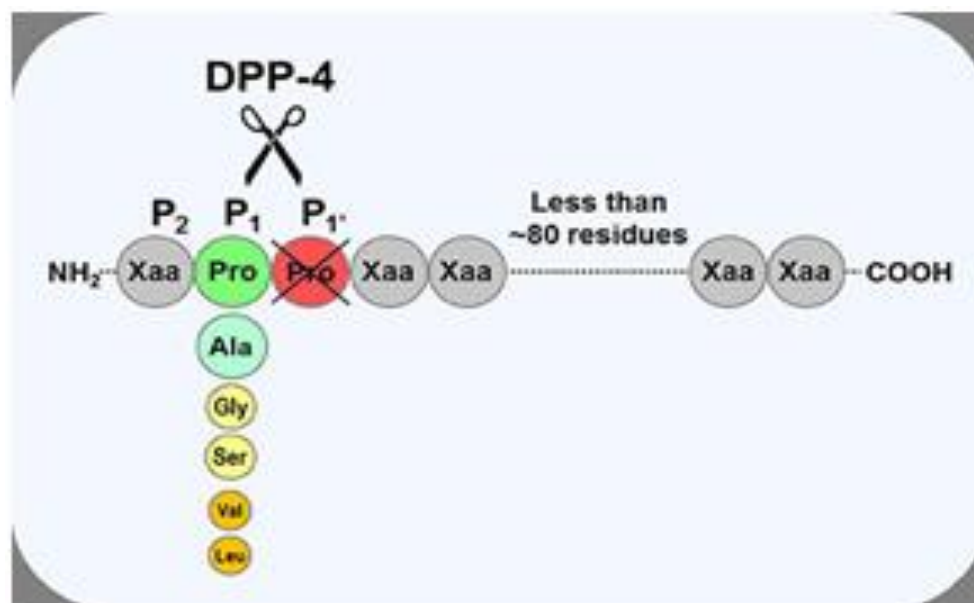


**Figure 1:** Substrate specificity of DPP-4, an amino peptidase called DPP-4 releases dipeptides from their substrates. Proline or alanine is preferred as the penultimate N-terminal residue in peptides or short proteins (below 80–100 residues), while certain substrates containing glycine, serine, valine, or leucine may still be cleaved at a slower rate. Proline at position three of the substrate prevents the enzyme from cleaving it [28].

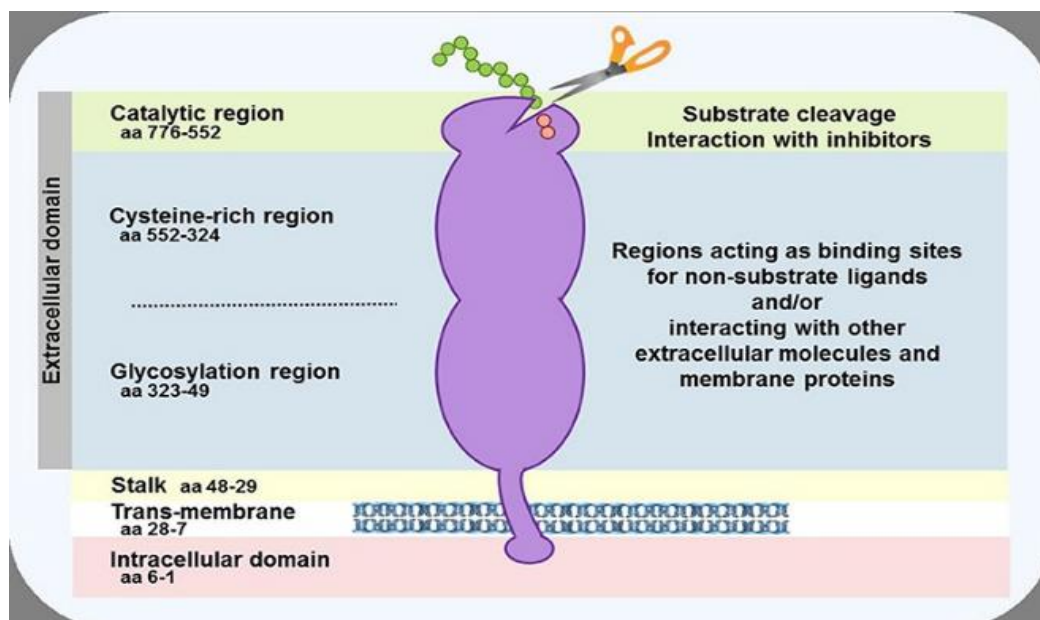


**Figure 2:** Shows the DPP-4 protein schematically. Two DPP-4 monomers dimerize to create a homodimer in the cell membrane. The soluble form of DPP-4, which circulates in the plasma, may be released when the monomers are split at the stalk. The catalytic pocket, which is created by residues containing serine at position 630 in the protein C-terminal region, houses the enzymatic activity. For several molecules, such as adenosine deaminase, caveolin-1, collagen, fibronectin, chemokine CXCR4 receptor, CD45, and sodium-hydrogen exchanger-3, sites within the cysteine-rich and glycosylation areas act as a receptor or ligand to mediate the non-enzymatic actions of the protein [28].

### Receptor grid generation

The protein gem structure, which was created using the protein preparation wizard, included the co-crystallized ligand and was used to create the receptor lattice. In order to describe the centroid of the dynamic docking location, a Grid box was created. The Glide grid generating wizard is used to create the Grid box. The protein Glide grid box dimensions, which represent the centroid of a docked posture, were set at 14\*14 \*14.

### Ligand preparation

The ligand structures were created using a 2D sketcher and then send to the LigPrep module of the Schrodinger suite 2020. The stereo concoction, ionisation, tautomeric variations, energy minimization and optimization for their shape, desalination, and correction for their chiralities and missing hydrogen atoms allowed the ligands to be converted from 2D to 3D structures. Using the Epik module, the ionisation and tautomeric states were generated within a pH range of 6.8 and 7.2. Mixtures were restricted using the OPLS-3 power field in the Impact bundle of Schrodinger during the last stage of LigPrep until a root mean square deviation of 1.8Å was achieved. Each ligand was given a single low-energy ring affirmation, and the streamlined ligands were then used for docking research.

### Glide ligand docking

By applying the Glide module of the Schrödinger suite 2020-3, the ligands RSMS1–50 are docked into the synergist pocket of the DPP-IV protein (PDB ID: 6B1E). Based on their Glide score, ligands are selected that are best-docked. The Glide ligand docking module was used to rate the successful interactions between the ligands and the receptor. OPLS-3 power field and extra precision (XP) mode were used for the docking. The docking procedure described above was carried out in flexible docking mode, which creates conformations for each input ligand automatically. This computation penalises steric conflicts while perceiving positive hydrogen-bonding, metal-ligation, and lipophilic connections. Finally, the constrained positions were rescored using the scoring capabilities of Glide Score. The docking results were examined using the XP visualizer of the Glide module. The Glide score of the common compound including Vildagliptin and Sitagliptin were compared to the score of dynamic molecules. Majority of the time, the Gide scoring capability depends on docking features like lipophilic persistence, where the ligands are encapsulated in the lipophilic pocket that is crucial for controlling the activity. Another parameter to increase the binding affinity is hydrogen bonding with various ligands and electrostatic forces. The mobility will be reduced by several unfavourable characteristics, such as XP penalties, rotational penalties, and so on. The QikProp module of Schrodinger suit-2020.

### Binding free energy calculation by using Prime/MM-GBSA approach

Molecular Mechanics-Generalized Born Surface Area (MM-GBSA) processes the binding free energies of the protein ligand complex using Schrödinger Suite 2020-3 Prime module, which integrates the OPLS3 power field and VSGB solvation model to examine computations.

**Table 1: Docking studies for compounds RSMS 1-50 with DPP-IV (6B1E)**

| Compounds    | D. Score | Lipophilic EvdW | PhobEn | H Bond | XP Electro | Low MW | Rot Penal | XP Penalties |
|--------------|----------|-----------------|--------|--------|------------|--------|-----------|--------------|
| RSMS1        | -5.35    | -2.54           | -0.35  | -1.36  | -0.79      | -0.46  | 0.24      | 0            |
| RSMS2        | -5.34    | -2.56           | -0.35  | -1.33  | -0.67      | -0.46  | 0.24      | 0            |
| RSMS3        | -5.11    | -1.91           | -0.55  | -1.59  | -0.72      | -0.5   | 0.18      | 0            |
| RSMS4        | -5.1     | -2.17           | -0.42  | -1.83  | -0.7       | -0.46  | 0.16      | 0            |
| RSMS5        | -5.11    | -4.99           | -0.55  | -1.32  | -0.72      | -0.5   | 0.16      | 0            |
| RSMS6        | -4.87    | -2.05           | -0.57  | -1.32  | -0.86      | -0.5   | 0.1       | 0            |
| RSMS7        | -5.11    | -5.11           | -0.76  | -1.57  | -1.14      | -0.32  | 0.32      | 0            |
| RSMS8        | -4.81    | -2.59           | -0.35  | -0.74  | -1.01      | -0.32  | 0.2       | 0.01         |
| RSMS9        | 4.98     | -2.09           | -0.51  | -1.78  | -0.65      | -0.42  | 0.15      | 0            |
| RSMS10       | -6.18    | -2.94           | -1.4   | -1.33  | -0.42      | -0.34  | 0.2       | 0.05         |
| RSMS11       | -7.05    | -3.25           | -1.05  | -1.34  | -1.4       | -0.24  | 0.23      | 0            |
| RSMS12       | -5.79    | -1.74           | -0.5   | -2.39  | -0.93      | -0.5   | 0.26      | 0            |
| RSMS13       | -4.49    | -2.03           | -0.38  | -1.84  | -0.71      | -0.36  | 0.14      | 0            |
| RSMS14       | -5.83    | -2.48           | -1.22  | -1.11  | -0.77      | -0.16  | 0.16      | 0            |
| RSMS15       | -6.46    | -2.16           | -0.71  | -2.45  | -1.07      | -0.36  | 0.28      | 0            |
| RSMS16       | -5.15    | -5.15           | -0.36  | -1.7   | -0.52      | -0.3   | 0.19      | 0.38         |
| RSMS17       | -4.52    | -4.75           | -1.13  | -0.59  | -0.35      | -0.38  | 0.22      | 0            |
| RSMS18       | -5.28    | -5.28           | 0      | -1.52  | -1.15      | -0.24  | 0.17      | 0.03         |
| RSMS19       | -5.46    | -3.18           | -0.62  | -0.7   | -0.59      | -0.3   | 0.25      | 0            |
| RSMS20       | -3.79    | -2.47           | 0      | -1.54  | -0.3       | -0.19  | 0.16      | 0.65         |
| RSMS21       | -4.49    | -2.2            | 0      | -1.43  | -0.77      | -0.29  | 0.19      | 0.09         |
| RSMS22       | -5.71    | -2.52           | -0.55  | -2.12  | -0.65      | -0.19  | 0.16      | 0.22         |
| RSMS23       | -5.69    | -2.5            | -0.44  | -1.33  | -0.43      | -0.2   | 0.17      | 0            |
| RSMS24       | -5.85    | -2.68           | -0.48  | -2.15  | -0.6       | -0.15  | 0.15      | 0            |
| RSMS25       | -5.69    | -2.58           | -0.4   | -2.17  | -0.58      | -0.1   | 0.14      | 0            |
| RSMS26       | -8.02    | -2.35           | -0.72  | -1.26  | -0.45      | -0.09  | 0.14      | 0            |
| RSMS27       | -5.41    | -2.61           | -0.33  | -1.82  | -0.68      | -0.1   | 0.14      | 0            |
| RSMS28       | -4.74    | -2.03           | 0      | -1.82  | -0.64      | -0.1   | 0.17      | 0            |
| RSMS29       | -5.72    | -2.79           | -5.71  | -1.15  | -0.91      | -0.15  | 0.15      | 0            |
| RSMS30       | -5.78    | -2.15           | -0.65  | -1.55  | -1.18      | -0.21  | 0.22      | 0            |
| RSMS31       | -5.73    | -2.15           | -0.65  | -1.22  | -0.72      | -0.21  | 0.22      | 0            |
| RSMS32       | -4.9     | -2.7            | -0.5   | -1.34  | -0.46      | -0.18  | 0.21      | 1            |
| RSMS33       | -5.4     | -2.39           | -0.97  | -1     | -0.71      | -0.24  | 0.23      | 0            |
| RSMS34       | -5.51    | -5.51           | -0.77  | -1.14  | -0.64      | -0.1   | 0.19      | 0            |
| RSMS35       | -6.17    | -2.55           | -1.26  | -1.08  | -1.02      | -0.15  | 0.21      | 0            |
| RSMS36       | -5.45    | -2.61           | -0.25  | -1.55  | -0.72      | -0.2   | 0.17      | 0.07         |
| RSMS37       | -4.94    | -2.59           | 0      | -1.61  | -0.74      | -0.16  | 0.21      | 0.35         |
| RSMS38       | -5.79    | -2.46           | -0.76  | -1.8   | -0.94      | -0.2   | 0.21      | 0.02         |
| RSMS39       | -3.75    | -2.55           | -0.26  | -1.78  | -0.69      | -0.15  | 0.21      | 1.38         |
| RSMS40       | -4.52    | -2.89           | -0.9   | -1.12  | -0.72      | -0.11  | 0.24      | 3.31         |
| RSMS41       | -4.32    | -1.34           | 0      | -2     | -0.97      | -0.26  | 0.18      | 0            |
| RSMS42       | -5.31    | -1.57           | -0.15  | -1.71  | -0.9       | -0.14  | 0.15      | 0            |
| RSMS43       | -5.35    | -2.28           | 0      | -1.33  | -0.85      | -0.03  | 0.13      | 1            |
| RSMS44       | -5.82    | -1.62           | -1.46  | -2.54  | -0.97      | -0.2   | 0.16      | 0            |
| RSMS45       | -8.39    | -3.01           | -1.56  | -2.34  | -0.73      | -0.03  | 0.13      | 0            |
| RSMS46       | -4.63    | -2.8            | -4.77  | -1.24  | -0.66      | -0.19  | 0.16      | 0            |
| RSMS47       | -6.9     | -3.07           | -1.64  | -0.72  | -0.66      | -0.11  | 0.15      | 0            |
| RSMS48       | -5.61    | -2.77           | -0.48  | -0.76  | -0.85      | -0.26  | 0.18      | 0            |
| RSMS49       | -2.2     | -2.46           | -0.23  | -0.98  | -0.87      | -0.19  | 0.16      | 2.4          |
| RSMS50       | -4.71    | -2.05           | -0.43  | -1.76  | -0.64      | -0.22  | 0.17      | 0            |
| Vildagliptin | -5.3     | -2.0            | -1.6   | -0.8   | -0.5       | -0.5   | 0.3       | 0            |
| Sitagliptin  | -5.6     | -1.6            | -1.6   | -0.6   | -0.6       | -0.2   | 0.2       | 0            |

## RESULTS AND DISCUSSION

To determine the coupling affinities of the ligands, the intended molecules were sub-atomically docked to the protein dynamic targets using the advanced sub-atomic docking software Schrodinger suit2020-3. To determine the structured analogues DPP-IV (6B1E) inhibitory effect against diabetes mellitus, the DPP-IV is docked with the analogues. When compared to ordinary Vildagliptin subsidiary with antidiabetic movement Vildagliptin and against antidiabetic drug Sitagliptin, the compounds RSMS 1-50 (Figure 1) showed remarkable receptor affinity. Table 1 displays the Glide scores from docking experiments against the DPP-IV receptor (PDB id 6B1E). When compared to conventional Vildagliptin (- 5.3) and Sitagliptin(-5.6), compounds RSMS 1–50, with the exception of RSMS 20,39,49, show substantial Glide scores in the range of – 4.32 to – 8.39. Because there are groups like cyano and aromatic rings present, the docking data show that the binding affinity is mostly caused by lipophilic components. In docking scores in the majority of the mixes, lipophilic factors have a significant role. In the vicinity of the Ser 630, Glu 205, and Glu 206 build-ups, which is the active site region, the cooperatives are practically overburdened (Figure 4). Figure 5 displays the developed ligands in their optimal docking postures. In Figure 6 the compounds with the highest Glide scores, RSMS 10, 15, 25, 26, 35, and 47, are presented in their best-docked positions. Figure 7 depicts the hydrogen bonding that the ligand RSMS 28 displayed with SER630 (H-bond length: 1.96 Å).

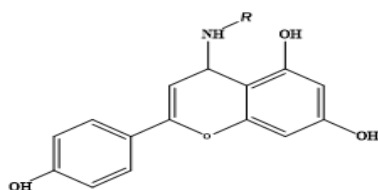


Figure 3: Structures of compounds RSMS 1-50

8-Amino substituted apigenin derivatives (1-50)

| S.No | R  |    | R |    | R |
|------|--|----|---|----|---|
| 1    | H <sub>3</sub> CH <sub>2</sub> CHCN                | 17 |   | 34 |   |
| 2    | H <sub>3</sub> C(H <sub>2</sub> C) <sub>2</sub> HN | 18 |   | 35 |   |
| 3    | (H <sub>3</sub> C) <sub>2</sub> HCHN               | 19 |   | 36 |   |
| 4    | (3HC) <sub>3</sub> HCHN                            | 20 |   | 37 |   |
| 5    | (H <sub>3</sub> C) <sub>2</sub> N                  | 21 |   | 38 |   |
| 6    | (C <sub>2</sub> H <sub>5</sub> ) <sub>2</sub> N    | 22 |   | 39 |   |
| 7    | (C <sub>3</sub> H <sub>7</sub> ) <sub>2</sub> N    | 23 |   | 40 |   |
| 8    |  | 24 |   | 41 |   |
| 9    |  | 25 |   | 42 |   |
| 10   |  | 26 |   | 43 |   |
| 11   |  | 27 |   | 44 |   |
| 12   |  | 29 |   | 45 |   |
| 13   |  | 30 |   | 46 |   |
| 14   |  | 31 |   | 47 |   |
| 15   |  | 32 |   | 48 |   |
| 16   |  | 33 |   | 49 |   |
|      |  |    |   | 50 |   |

6B1E - minimized - RSMS25.mol

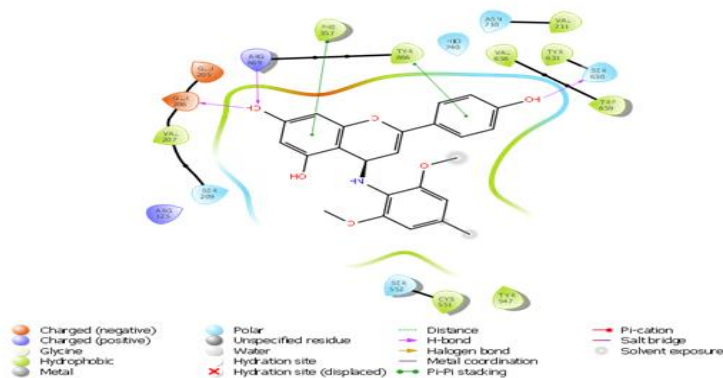


Figure 4: Ligand interaction of compound RSMS25 with DPP-IV (6B1E)





**Table 2: Insilico ADMET screening for proposed compounds (RSMS1-50)**

| Compounds          | Mol. Wt | Dipole | Donor HB | Accept HB | QPlog o/w | #metab | Rule of five | %Human oral absorption       |
|--------------------|---------|--------|----------|-----------|-----------|--------|--------------|------------------------------|
| RSMS1              | 313.352 | 2.644  | 4        | 4.250     | 2.060     | 5      | 0            | 73.205                       |
| RSMS2              | 313.352 | 2.644  | 4        | 4.250     | 2.060     | 5      | 0            | 73.205                       |
| RSMS3              | 299.326 | 2.141  | 4        | 4.250     | 1.604     | 5      | 0            | 69.738                       |
| RSMS4              | 313.352 | 2.329  | 4        | 4.250     | 1.839     | 5      | 0            | 71.850                       |
| RSMS5              | 299.326 | 2.141  | 4        | 4.250     | 1.604     | 5      | 0            | 69.738                       |
| RSMS6              | 285.299 | 2.116  | 4        | 4.250     | 1.173     | 5      | 0            | 65.595                       |
| RSMS7              | 355.433 | 2.391  | 4        | 4.250     | 3.005     | 5      | 0            | 79.191                       |
| RSMS8              | 355.433 | 2.380  | 4        | 4.250     | 2.564     | 4      | 0            | 78.935                       |
| RSMS9              | 323.348 | 2.371  | 3        | 4.750     | 2.142     | 6      | 0            | 74.969                       |
| RSMS10             | 347.370 | 4.615  | 4        | 3.750     | 3.286     | 7      | 0            | 91.180                       |
| RSMS11             | 377.396 | 4.356  | 5        | 5.00      | 2.397     | 7      | 0            | 70.926                       |
| RSMS12             | 301.298 | 3.979  | 5        | 5.950     | 0.187     | 6      | 0            | 50.080                       |
| RSMS13             | 341.363 | 4.106  | 3        | 6.450     | 1.558     | 5      | 0            | 72.059                       |
| RSMS14             | 401.341 | 4.243  | 4        | 3.750     | 3.887     | 5      | 0            | 95.466                       |
| RSMS15             | 343.335 | 0.896  | 5        | 6.250     | -0.651    | 6      | 0            | 34.281                       |
| RSMS16             | 361.396 | 4.421  | 4        | 3.750     | 3.585     | 6      | 0            | 92.938                       |
| RSMS17             | 335.359 | 5.159  | 4        | 3.750     | 2.498     | 6      | 0            | 75.685                       |
| RSMS18             | 377.396 | 4.660  | 4        | 4.500     | 3.417     | 7      | 0            | 91.938                       |
| RSMS19             | 361.396 | 2.267  | 4        | 4.250     | 2.904     | 6      | 0            | 78.449                       |
| RSMS20             | 392.367 | 12.070 | 4        | 4.750     | 2.632     | 6      | 0            | 77.780                       |
| RSMS21             | 363.369 | 4.860  | 5        | 4.50      | 2.509     | 7      | 0            | 77.375                       |
| RSMS22             | 393.395 | 6.224  | 5        | 4.250     | 2.697     | 8      | 0            | 78.946                       |
| RSMS23             | 389.450 | 2.875  | 4        | 3.750     | 4.088     | 8      | 0            | 100                          |
| RSMS24             | 405.449 | 3.037  | 4        | 4.500     | 4.086     | 9      | 0            | 100                          |
| RSMS25             | 421.449 | 2.939  | 4        | 5.250     | 3.950     | 9      | 0            | 95.891                       |
| RSMS26             | 423.421 | 2.377  | 5        | 6.00      | 2.884     | 8      | 0            | 80.343                       |
| RSMS27             | 419.476 | 3.070  | 4        | 4.50      | 4.395     | 9      | 0            | 100                          |
| RSMS28             | 389.450 | 2.802  | 4        | 3.750     | 4.050     | 9      | 0            | 100                          |
| RSMS29             | 405.449 | 2.909  | 5        | 4.500     | 3.424     | 9      | 0            | 89.235                       |
| RSMS30             | 386.406 | 6.165  | 4        | 5.250     | 2.958     | 6      | 0            | 77.855                       |
| RSMS31             | 386.406 | 3.758  | 4        | 5.250     | 2.495     | 6      | 0            | 77.213                       |
| RSMS32             | 395.841 | 4.966  | 4        | 4.250     | 3.350     | 6      | 0            | 81.417                       |
| RSMS33             | 379.387 | 3.563  | 4        | 4.250     | 3.116     | 6      | 0            | 79.400                       |
| RSMS34             | 420.851 | 1.822  | 4        | 5.250     | 3.214     | 6      | 0            | 81.212                       |
| RSMS35             | 404.397 | 3.264  | 4        | 5.250     | 2.683     | 6      | 0            | 77.888                       |
| RSMS36             | 389.407 | 7.889  | 4        | 5.750     | 2.872     | 6      | 0            | 79.808                       |
| RSMS37             | 403.434 | 7.423  | 4        | 5.750     | 3.197     | 5      | 0            | 83.050                       |
| RSMS38             | 390.395 | 8.776  | 6        | 6.250     | 1.691     | 6      | 0            | 49.995                       |
| RSMS39             | 404.421 | 8.261  | 5        | 6.250     | 2.700     | 5      | 0            | 78.042                       |
| RSMS40             | 416.432 | 7.966  | 4        | 5.750     | 3.321     | 5      | 0            | 82.915                       |
| RSMS41             | 372.379 | 5.699  | 4        | 5.250     | 2.681     | 6      | 0            | 77.269                       |
| RSMS42             | 406.824 | 7.414  | 4        | 5.250     | 3.155     | 6      | 0            | 80.921                       |
| RSMS43             | 440.378 | 9.457  | 4        | 5.250     | 3.641     | 6      | 0            | 84.812                       |
| RSMS44             | 390.370 | 5.824  | 4        | 5.250     | 2.777     | 4      | 0            | 80.165                       |
| RSMS45             | 440.378 | 7.947  | 4        | 5.250     | 3.645     | 5      | 0            | 82.915                       |
| RSMS46             | 393.355 | 8.194  | 4        | 5.250     | 2.322     | 7      | 0            | 68.400                       |
| RSMS47             | 416.356 | 4.799  | 4        | 4.250     | 3.936     | 6      | 0            | 94.448                       |
| RSMS48             | 373.367 | 4.461  | 4        | 5.250     | 2.990     | 6      | 0            | 88.318                       |
| RSMS49             | 393.355 | 6.774  | 4        | 5.250     | 2.434     | 6      | 0            | 73.140                       |
| RSMS50             | 382.802 | 3.289  | 4        | 4.250     | 3.413     | 5      | 0            | 91.371                       |
| Vildagliptin       | 303.43  | 6.322  | 2        | 6.750     | 0.438     | 4      | 0            | 59.478                       |
| Sitagliptin        | 393.291 | 4.456  | 2        | 6         | 2.24      | 5      | 0            | 75.455                       |
| Recommended Values | 13.-725 | 1-12.5 | 0-6      | 2-20      | -2-6.5    | 1-8    | Max 4        | >80% is high<br><25% is poor |

MW- Molecular weight of the molecule,

Dipole – Computed dipole moment

donorHB - Estimated number of hydrogen bonds that would be donated by the solute to water molecules in an aqueous solution.

accptHB- Estimated number of hydrogen bonds that would be accepted by the solute from water molecules in an aqueous solution

QPlogPo/w - Predicted octanol/water partition coefficient.

#metab- Number of likely metabolic reactions.

RuleOfFive Number of violations of Lipinski's rule of five.

%Human- Oral absorption- Predicted human oral absorption on 0 to 100% scale.

**Table 3: Binding free energy calculation using Prime/MM-GBSA approach**

| Compounds    | $\Delta G$ bind (Kcal/mol) | $\Delta G$ bind columb | $\Delta G$ bind covalent | $\Delta G$ bind vander | $\Delta G$ Bind H Bond | $\Delta G$ bind Lipophilic |
|--------------|----------------------------|------------------------|--------------------------|------------------------|------------------------|----------------------------|
| RSMS1        | -13.80                     | -26.59                 | 8.64                     | -36                    | -1.68                  | -14.43                     |
| RSMS2        | -13.80                     | -16.98                 | 8.01                     | -36.62                 | -1.69                  | -14.43                     |
| RSMS3        | -24.89                     | -26.39                 | 8.25                     | -35.56                 | -1.82                  | -15.43                     |
| RSMS4        | -16.38                     | -29.16                 | 6.72                     | -34.13                 | -1.5                   | -16.38                     |
| RSMS5        | -17.83                     | -26.41                 | 8.29                     | -35.33                 | -2.21                  | -15.12                     |
| RSMS6        | -15.78                     | -27.11                 | 2.2                      | -33.32                 | -2.18                  | -14.17                     |
| RSMS7        | -20.68                     | -33.61                 | 7.16                     | -29.75                 | -2.57                  | -19.71                     |
| RSMS8        | -2.75                      | -23.51                 | 2.1                      | -39.25                 | -1.55                  | -18.66                     |
| RSMS9        | -10.22                     | -24.87                 | 7.5                      | -34.75                 | -1.5                   | -19.83                     |
| RSMS10       | -21.59                     | -13.13                 | 5.96                     | -26.96                 | -1.44                  | -16.05                     |
| RSMS11       | -18.81                     | -27.16                 | 3.07                     | -40.95                 | -2.07                  | -23.26                     |
| RSMS12       | -20.64                     | -35.27                 | 3.8                      | -27.4                  | -3.61                  | -20.76                     |
| RSMS13       | -23.24                     | -24.61                 | 5.84                     | -34.86                 | -2.25                  | -14.53                     |
| RSMS14       | -5.85                      | -31.93                 | 2.66                     | -37.76                 | -2.23                  | -17.85                     |
| RSMS15       | -24.22                     | -25.76                 | 6.72                     | -34.23                 | -3.14                  | -11.48                     |
| RSMS16       | -14.82                     | -11.82                 | 7.21                     | -39.61                 | -1.86                  | -20.5                      |
| RSMS17       | -19.45                     | -21.03                 | 2.81                     | -30.55                 | -1.46                  | -17.66                     |
| RSMS18       | -17.67                     | -30.81                 | 7.81                     | -41.08                 | -2.15                  | -22.32                     |
| RSMS19       | -24.97                     | -26.1                  | 2.61                     | -37.08                 | -1.38                  | -22.31                     |
| RSMS20       | -36.45                     | -17.03                 | 7.36                     | -46.04                 | -2.05                  | -19.13                     |
| RSMS21       | -13.47                     | -37.23                 | 10.08                    | -30.16                 | -3.95                  | -21.81                     |
| RSMS22       | -24.21                     | -21.52                 | 9.44                     | -47.5                  | -2.65                  | -21.97                     |
| RSMS23       | 18.25                      | -26.49                 | 5.26                     | -41.42                 | -1.58                  | -26.03                     |
| RSMS24       | -23.96                     | -13.37                 | 4.91                     | -42.77                 | -2.14                  | -21.26                     |
| RSMS25       | -24.07                     | -10.48                 | 7.99                     | -45.62                 | -2.2                   | -20.97                     |
| RSMS26       | 6.42                       | -50.72                 | 11.85                    | -40.69                 | -1.28                  | -18.99                     |
| RSMS27       | -22.04                     | -9.33                  | 6.33                     | -49.2                  | -1.43                  | -18.51                     |
| RSMS28       | -15.96                     | -23.11                 | 3.67                     | -37.73                 | -2.22                  | -18.75                     |
| RSMS29       | -30.31                     | -33.9                  | 8                        | -39.79                 | -2.18                  | -24.66                     |
| RSMS30       | -46.23                     | -17.79                 | 3.32                     | -43.74                 | -2.66                  | -20.34                     |
| RSMS31       | -32.41                     | -17.71                 | 4.41                     | -36.47                 | -1.49                  | -22.42                     |
| RSMS32       | -30.02                     | -24.86                 | 5.31                     | -36.62                 | -1.65                  | -20.56                     |
| RSMS33       | -22.27                     | -32.81                 | 1.77                     | -38.32                 | -2.3                   | -22.75                     |
| RSMS34       | -14.84                     | -12.26                 | 4.06                     | -38.06                 | -1.78                  | -18.33                     |
| RSMS35       | -22.54                     | -15.42                 | 4.74                     | -36.01                 | -1.34                  | -21                        |
| RSMS36       | -26.59                     | -19.51                 | 10.56                    | -43.77                 | -2.03                  | -19.25                     |
| RSMS37       | -22.21                     | -32.43                 | 8.22                     | -43.26                 | -2.78                  | -15.81                     |
| RSMS38       | -31.79                     | -41.22                 | 10.91                    | -36.8                  | -1.7                   | -19                        |
| RSMS39       | -16.34                     | -19.17                 | 8.84                     | -44.57                 | -2.33                  | -15.03                     |
| RSMS40       | -26.52                     | -20.06                 | 8.43                     | -46.56                 | -2.19                  | -21.42                     |
| RSMS41       | -22.54                     | -34                    | 7.18                     | -34.08                 | -2.56                  | -15.13                     |
| RSMS42       | -31.24                     | -34                    | 8.81                     | -39.87                 | -2.82                  | -19.67                     |
| RSMS43       | -29.77                     | -31                    | 5.6                      | -36.14                 | -1.51                  | -19.81                     |
| RSMS44       | -15.61                     | -35.89                 | 2.77                     | -29.54                 | -3.15                  | -18.87                     |
| RSMS45       | -18                        | -37.39                 | 9.88                     | -42.28                 | -2.56                  | -15.33                     |
| RSMS46       | -28.37                     | -0.32                  | 6.03                     | -42.58                 | -2.18                  | -17.25                     |
| RSMS47       | -8.33                      | -14.02                 | 3.59                     | -41.07                 | -1.26                  | -16.13                     |
| RSMS48       | -24.75                     | -8.29                  | 8.54                     | -40.15                 | -2.19                  | -16.43                     |
| RSMS49       | -26.02                     | -14.7                  | 8.94                     | -45.02                 | -3.53                  | -16.64                     |
| RSMS50       | -10.08                     | -23.11                 | 8.02                     | -38.57                 | -1.25                  | -22                        |
| Sitagliptin  | -18.2                      | -20.31                 | 3.05                     | -33.79                 | -1.63                  | -13.89                     |
| Vildagliptin | -10.85                     | -32.05                 | 0.02                     | -31.07                 | -1.96                  | -16.37                     |

By applying the qikprop module of the Schrödinger suite 2020-3, the ADMET characteristics for the planned ligands RMMS1–50 may be foreseen in-silico. Compounds with molecular weights between 285 and 440. The molecules processed dipole moments range from 1.822 to 12.070. In a fluid configuration of the mixtures, it is estimated that the solute would provide 2–6 hydrogen bonds to the water atoms. The range of 3.750 to 6.750 is the estimated number of hydrogen bonds that would be recognised by the solute from water particles in a fluid arrangement of the compounds. The compounds QPlogP values are the highest. There are a variety of 4–8 possible metabolic reactions to the chemicals. There have been 0 instances of Lipinski's rule of five being broken. Human oral absorption of the substance's ranges from 75 to 100%. According to the in-silico ADMET screening findings, the majority of the chemicals fall within the advised ranges. Table 2 illustrates the finer points of the ADMET characteristics for compounds RSMS1–50. Additionally, MM-GBSA free restricting vitality, which is discovered using the post scoring technique for the DPP-IV (PDB ID: 6B1E) target, was used to evaluate molecular docking. Examining the lowest energy postures predicted by the scoring function demonstrates the accuracy of docking. The experimental binding mode identified by X-ray crystallography and the Glide scores match one other nearly perfectly. The docking of ligands into the coupling pocket

results in the Glide score and MM-GBSA free energy values. Table 3 illustrates the intricacies of the MM-GBSA free restricting vitality for the compounds RSMS1-50.

## CONCLUSION

Generally, 8-Amino apigenin analogues demonstrated a variety of biological actions, including the ability to fight off bacteria and treat diabetes. According to the molecular docking investigation, 8-Amino apigenin analogues showed improved organisation at dynamic site by interacting with multiple amino along with cyano corrosive build-ups. In this manner, the in-silico structuring approach used in the current study assisted in identifying the lead atoms and may also aid to partially explain their helpful influence for further tests like in vitro and in vivo evaluation. Based on this assumption, researchers recently shown that the 8-Amino apigenin analogues arrangement used DPP-IV enzyme restraint as harmful to antidiabetic action. The in-silico study's findings clearly showed that a large number of the 8-Amino apigenin analogues family may demonstrate fascinating anti-diabetic activity. After further refining, the compounds RSMS 10, 15, 35, 26, 30, 45, and 47 are likely to be useful analogues since they exhibit strong DPP-IV Inhibitory anti-diabetic action with potential for remedy.

## ETHICS APPROVAL AND CONSENT TO PARTICIPATE

Not applicable.

## HUMAN AND ANIMAL RIGHTS

No animals/humans were used for studies that are the basis of this research.

## CONSENT FOR PUBLICATION

Not applicable.

## AVAILABILITY OF DATA AND MATERIALS

Not applicable.

## FUNDING

RGPV RDF Fellowship.

## CONFLICT OF INTEREST

The authors declare no conflict of interest, financial or otherwise.

## ACKNOWLEDGEMENTS

The authors express their sincere gratitude to School of Pharmaceutical Sciences, Rajiv Gandhi Proudyogiki Vishwavidyalaya, Bhopal for technical support.

## REFERENCES

1. Zimmet P, Alberti KG, Shaw J. Global and societal implications of the diabetes epidemic. *Nature*. 2001; 414(6865):782-7.
2. Mokdad AH, Ford ES, Bowman BA, Dietz WH, Vinicor F, Bales VS, Marks JS. Prevalence of obesity, diabetes, and obesity-related health risk factors, 2001. *Jama*. 2003; 289(1):76-9.
3. Krentz AJ, Patel MB, Bailey CJ. New drugs for type 2 diabetes mellitus. *Drugs*. 2008; 68(15):2131-62.
4. Phung OJ, Scholle JM, Talwar M, Coleman CI. Effect of noninsulin antidiabetic drugs added to metformin therapy on glycemic control, weight gain, and hypoglycemia in type 2 diabetes. *Jama*. 2010; 303(14):1410-8.
5. Monami M, Cremasco F, Lamanna C, Marchionni N, Mannucci E. Predictors of response to dipeptidyl peptidase-4 inhibitors: evidence from randomized clinical trials. *Diabetes/Metabolism Research and Reviews*. 2011; 27(4):362-72.
6. Bennett WL, Maruthur NM, Singh S, Segal JB, Wilson LM, Chatterjee R, Marinopoulos SS, Puhon MA, Ranasinghe P, Block L, Nicholson WK. Comparative effectiveness and safety of medications for type 2 diabetes: an update including new drugs and 2-drug combinations. *Annals of Internal Medicine*. 2011; 154(9):602-13.
7. Scheen AJ. A review of gliptins in 2011. *Expert Opinion on Pharmacotherapy*. 2012; 13(1):81-99.
8. Neumiller JJ, Wood L, Campbell RK. Dipeptidyl peptidase-4 inhibitors for the treatment of type 2 diabetes mellitus. *Pharmacotherapy*. 2010; 30:463-484.
9. Halperin I, Ma B, Wolfson H, Nussinov R. Principles of docking: An overview of search algorithms and a guide to scoring functions. *Proteins: Structure, Function, and Bioinformatics*. 2002; 47(4):409-43.
10. Jagan K, Radika MK, Priyadarshini E, Venkatraman C. A study on the inhibitory potential of DPP-IV enzyme by apigenin through in silico and in vivo approaches. *Research Journal of Recent Sciences*. 2015; 4:22-29.
11. Jiang J, Tang T, Peng Y, Liu M, Liu Q, Mi P, Yang Z, Chen H, Zheng X. Research progress on antidiabetic activity of apigenin derivatives. *Medicinal Chemistry Research*. 2022:1-1.
12. Li N, Wang LJ, Jiang B, Li XQ, Guo CL, Guo SJ, Shi DY. Recent progress of the development of dipeptidyl peptidase-4 inhibitors for the treatment of type 2 diabetes mellitus. *European Journal of Medicinal Chemistry*. 2018; 151:145-57.
13. Cheng N, Yi WB, Wang QQ, Peng SM, Zou XQ. Synthesis and  $\alpha$ -glucosidase inhibitory activity of chrysin, diosmetin, apigenin, and luteolin derivatives. *Chinese Chemical Letters*. 2014; 25(7):1094-8.
14. Abbas G, Al Harrasi A, Hussain H, Hamaed A, Supuran CT. The management of diabetes mellitus-imperative role of natural products against dipeptidyl peptidase-4,  $\alpha$ -glucosidase and sodium-dependent glucose co-transporter 2 (SGLT2). *Bioorganic Chemistry*. 2019; 86:305-15.
15. Lacroix IM, Li-Chan EC. Overview of food products and dietary constituents with antidiabetic properties and their putative mechanisms of action: A natural approach to complement pharmacotherapy in the management of diabetes. *Molecular Nutrition & Food Research*. 2014; 58(1):61-78.

16. Tripuraneni NS, Azam MA. Pharmacophore modeling, 3D-QSAR and docking study of 2-phenylpyrimidine analogues as selective PDE4B inhibitors. *Journal of Theoretical Biology*. 2016; 394:117-26.
17. Lengauer T, Rarey M. Computational methods for biomolecular docking. *Current Opinion in Structural Biology*. 1996; 6(3):402-6.
18. Kalirajan R, Sankar S, Jubie S, Gowramma B. Molecular docking studies and in-silico ADMET screening of some novel oxazine substituted 9-anilinoacridines as topoisomerase II inhibitors. *Indian Journal of Pharmaceutical Education and Research*. 2017; 51(1):110-5.
19. Kalirajan R, Pandiselvi A, Gowramma B, Balachandran P. In-silico design, ADMET screening, MM-GBSA binding free energy of some novel isoxazole substituted 9-anilinoacridines as HER2 inhibitors targeting breast cancer. *Current Drug Research Reviews Formerly: Current Drug Abuse Reviews*. 2019; 11(2):118-28.
20. Li M, Bao X, Zhang X, Ren H, Cai S, Hu X, Yi J. Exploring the phytochemicals and inhibitory effects against  $\alpha$ -glucosidase and dipeptidyl peptidase-IV in Chinese pickled chili pepper: Insights into mechanisms by molecular docking analysis. *LWT*. 2022; 162:113467.
21. Singhal S, Singhal SP, Patil V. # 148 In silico ADME and toxicity prediction of resveratrol derivatives for DPP-4 inhibition activity: Molecular docking study. *Journal of Pharmaceutical Chemistry*. 2022; 8.
22. Mentlein R. Dipeptidyl-peptidase IV (CD26)-role in the inactivation of regulatory peptides. *Regulatory Peptides*. 1999; 85(1):9-24.
23. Demuth HU, McIntosh CH, Pederson RA. Type 2 diabetes-therapy with dipeptidyl peptidase IV inhibitors. *Biochimica et Biophysica Acta (BBA)-Proteins and Proteomics*. 2005; 1751(1):33-44.
24. Yu DM, Yao TW, Chowdhury S, Nadvi NA, Osborne B, Church WB, McCaughan GW, Gorrell MD. The dipeptidyl peptidase IV family in cancer and cell biology. *The FEBS Journal*. 2010; 277(5):1126-44.
25. Lambeir AM, Durinx C, Scharpé S, De Meester I. Dipeptidyl-peptidase IV from bench to bedside: an update on structural properties, functions, and clinical aspects of the enzyme DPP IV. *Critical Reviews in Clinical Laboratory Sciences*. 2003; 40(3):209-94.
26. Ohnuma K, Dang NH, Morimoto C. Revisiting an old acquaintance: CD26 and its molecular mechanisms in T cell function. *Trends in Immunology*. 2008; 29(6):295-301.
27. Hühn J, Ehrlich S, Fleischer B, von Bonin A. Molecular analysis of CD26-mediated signal transduction in T cells. *Immunology Letters*. 2000; 72(2):127-32.
28. Deacon CF. Physiology and pharmacology of DPP-4 in glucose homeostasis and the treatment of type 2 diabetes. *Frontiers in Endocrinology*. 2019; 10:80.